

# Sapphire Whispering Gallery Thermometer

G. F. Strouse

Published online: 3 October 2007  
© Springer Science+Business Media, LLC 2007

**Abstract** An innovative sapphire whispering gallery thermometer (SWGT) is being explored at the National Institute of Standards and Technology (NIST) as a potential replacement for a standard platinum resistance thermometer (SPRT) for industrial applications that require measurement uncertainties of  $\leq 10$  mK. The NIST SWGT uses a synthetic sapphire monocrystalline disk configured as a uniaxial, dielectric resonator with whispering gallery modes between 14 GHz and 20 GHz and with  $Q$ -factors as large as 90,000. The prototype SWGT stability at the ice melting point ( $0^\circ\text{C}$ ) is  $\leq 1$  mK with a frequency resolution equivalent to 0.05 mK. The prototype SWGT measurement uncertainty ( $k=1$ ) is 10 mK from  $0^\circ\text{C}$  to  $100^\circ\text{C}$  for all five resonance modes studied. These results for the SWGT approach the capabilities of industrial resistance thermometers. The SWGT promises greatly increased resistance to mechanical shock relative to SPRTs, over the range from  $-196^\circ\text{C}$  to  $500^\circ\text{C}$  while retaining the low uncertainties needed by secondary calibration laboratories. The temperature sensitivity of the SWGT depends upon a well-defined property (the refractive index at microwave frequencies) and the thermal expansion of a pure material. Therefore, it is expected that SWGTs can be calibrated over a wide temperature range using a reference function, along with deviations measured at a few fixed points. This article reports the prototype SWGT stability, resolution, repeatability, and the temperature dependence of five whispering gallery resonance frequencies in the range from  $0^\circ\text{C}$  to  $100^\circ\text{C}$ .

---

Certain commercial equipments, instruments or materials are identified in this article in order to adequately specify the experimental procedure. Such identification does not imply recommendation or endorsement by the NIST.

---

G. F. Strouse (✉)  
Process Measurements Division, National Institute of Standards and Technology, 100 Bureau Drive,  
MS 8363, Gaithersburg, MD 20899-8363, USA  
e-mail: gregory.strouse@nist.gov

**Keywords** Microwave oscillator · Resonance thermometer · Sapphire · Sapphire thermometer · Whispering gallery mode resonance · Whispering gallery mode resonator (WGMR)

## 1 Introduction

Since 1973, the whispering gallery mode resonator (WGMR) has been used as an ultra-stable resonator ( $\Delta f/f < 10^{-12}$  at  $-196^\circ\text{C}$ ), as described in [1–10] and in over 50 other references. Reference [10] provides an up-to-date overview (historical and future) of sapphire whispering gallery mode frequency standards. Synthetic sapphire monocrystalline disks that are configured as uniaxial anisotropic dielectric resonators exhibit  $Q$ -factors as large as 850,000 at  $-196^\circ\text{C}$ . These quasi-TM modes (whispering gallery modes) in a cylindrical disk have large electromagnetic fields near the cylindrical boundary. Much of the extant literature describes how to build a temperature-compensated WGMR (e.g., cryogenic cooling, multiple crystals, crystal shapes). To use the WGMR as a thermometer, we did not implement the temperature-compensating practices.

The intrinsic temperature dependence of the refractive index (or its near equivalent, the permittivity) of the synthetic sapphire, coupled with the ease of measuring the frequencies of high- $Q$  ( $>20,000$ ) resonant modes, allows the use of a sapphire WGMR as a thermometer rather than a frequency standard. The sapphire whispering gallery thermometer (SWGTT) comprises a synthetic sapphire monocrystalline disk configured as a uniaxial anisotropic dielectric resonator. Out of the infinite number of whispering gallery modes, we study those with resonant frequencies occurring between 14 GHz and 20 GHz, which exhibit  $Q$ -factors approaching 100,000 at  $0^\circ\text{C}$ . The frequency–temperature relationship is primarily due to the temperature dependence of the refractive index. The thermal expansion of the sapphire contributes approximately 10% to the sensitivity, whereas the thermal expansion of the enclosure contributes less than 0.3%. According to the literature, the resonance frequency of a  $c$ -axis cut sapphire crystal exhibits a temperature sensitivity of  $(df/dT)/f$  of  $-10 \times 10^6 \text{ }^\circ\text{C}^{-1}$  at  $-196^\circ\text{C}$  that increases to  $-50 \times 10^6 \text{ }^\circ\text{C}^{-1}$  at  $77^\circ\text{C}$  [2]. No extant literature investigates the frequency–temperature sensitivity above  $77^\circ\text{C}$ . Challenges for developing an SWGTT include developing a high- $Q$  resonator with small volume, understanding and avoiding possible effects from chemical contamination of the sapphire surface, and understanding any mechanisms that cause thermal hysteresis.

Currently, the standard platinum resistance thermometer (SPRT) is the thermometer of choice in the range from  $-196^\circ\text{C}$  to  $500^\circ\text{C}$  when measurement uncertainties  $\leq 10 \text{ mK}$  are required. The critical limitation of an SPRT in industrial applications is its sensitivity to mechanical shock in handling and shipping. Shocks change the physical state of the annealed, loosely supported platinum resistance element. These changes often prevent an SPRT from meeting the required measurement uncertainty. As shown in a recent key comparison and in a recent NIST article on SPRT stabilization, an equivalent change of 10 mK in the triple point of water resistance of an SPRT is common [11]. A shift of this magnitude is at least a factor of 20 greater than the calibration uncertainty, and it can cause an error the measurement of temperature by as much as

30 mK at high temperatures. This exceeds the required measurement uncertainty of  $<10$  mK. As compared to platinum, synthetic sapphire is thought to be mechanically more stable up to  $1800^\circ\text{C}$  and less subject to changes in physical state (e.g., oxidation, growth of crystal defects) [12, 13]. Due to the inherent stability issue of an SPRT, the SWGT represents a potential replacement for an SPRT in industrial applications where measurement uncertainty below 10 mK is required. This article quantifies the stability, resolution, and repeatability of one SWGT, and the temperature dependence of its whispering gallery resonance frequencies.

## 2 Theoretical Background

A monocrystalline sapphire disk is uniaxially anisotropic, where a crystal with a  $c$ -axis aligned in the  $z$ -direction exhibits high-order azimuthal modes (whispering gallery modes). If a pure whispering gallery mode existed in only the radial direction, then the frequency–temperature dependence due to changes in permittivity of the sapphire crystal can be expressed as

$$\frac{1}{f_0} \frac{\partial f_0}{\partial T} = \frac{1}{f} \left( \frac{\partial f_0}{\partial \varepsilon_\perp} \frac{\partial \varepsilon_\perp}{\partial T} + \frac{\partial f_0}{\partial \varepsilon_\parallel} \frac{\partial \varepsilon_\parallel}{\partial T} + \frac{\partial f_0}{\partial L} \frac{\partial L}{\partial T} + \frac{\partial f_0}{\partial a} \frac{\partial a}{\partial T} \right), \quad (1)$$

where  $f_0$  is the center resonance frequency,  $\varepsilon_\perp$  is the permittivity in the radial direction,  $\varepsilon_\parallel$  is the permittivity in the axial direction,  $L$  is the axial length of the sapphire disk, and  $a$  is the sapphire disk diameter with the assumption that the relative magnetic permeability is exactly one [2]. As sketched in Fig. 1, the whispering gallery resonances occur in the sapphire disk when standing waves are excited along the circumference of the disk with minimal reflection losses. For the quasi-TM modes of the SWGT, Eq. 1 may be reduced to estimate the frequency–temperature dependence relationship:

$$\frac{1}{f_0} \frac{\partial f}{\partial T} \approx -\frac{1}{2} \frac{1}{\varepsilon_\parallel} \frac{\partial \varepsilon_\parallel}{\partial T} - \alpha_\perp, \quad (2)$$

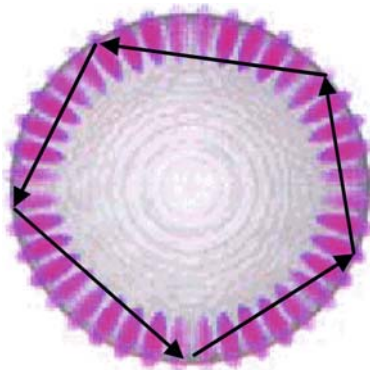


**Fig. 1** Whispering gallery mode resonance where the electromagnetic waves experience total internal reflection within the circumference of the monocrystalline sapphire disk

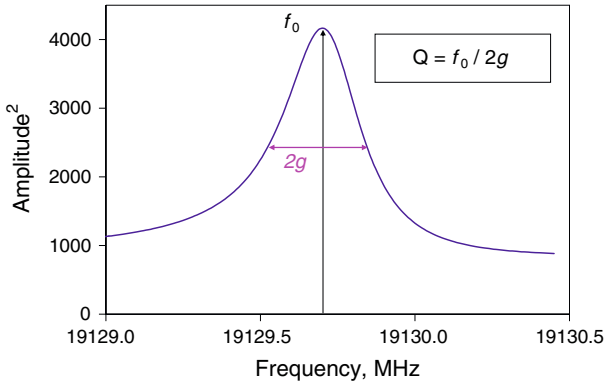


**Fig. 2**  $Q$ -factor determination for a resonance, where  $g$  is the half-width and  $f_0$  is the center frequency of the resonance

where  $\alpha_{\perp}$  is the thermal expansion in the radial direction [2,4].

The  $Q$ -factor (quality factor) of a resonance frequency is defined as:

$$Q = \frac{f_0}{2g}, \quad (3)$$

where  $g$  is the half-width defined as the width of  $f$  for which the energy is half the peak of the center resonance frequency  $f_0$  (see Fig. 2 for a graphical representation) [14].

### 3 SWGT Prototype Design

The NIST SWGT utilizes previously-published designs [1–10]; however, our design enhances the temperature sensitivity of the whispering gallery resonances. Three prototype SWGTs (SWGT-T1, -T2, and -T3) were designed such that each successive version was smaller in disk size and cavity volume. In order to optimize the whispering gallery resonances and minimize the SWGT size, the sapphire disk height was twice the disk radius and the cavity radius and height were twice the respective disk values [1]. The radii of the sapphire disks were 8.8, 5.9, and 4.4 mm for SWGT-T1, -T2, and -T3, respectively.

The SWGT disks were machined from HEMEX<sup>TM</sup>-grade single crystal synthetic sapphire ( $\alpha$ -Al<sub>2</sub>O<sub>3</sub>) with a  $c$ -axis orientation in the  $z$ -direction aligned to within  $\pm 0.1\%$ . A  $10^\circ$   $c$ -axis misalignment of the synthetic sapphire disk can decrease the  $Q$ -factor of the WGMR by as much as 15% [3]. A stainless-steel screw passing through a 2 mm diameter hole in the sapphire disk center supports the sapphire disk in the center of a coin-shaped, copper resonance cavity. Since the electromagnetic fields of a whispering gallery resonance are confined to a region near the circumference of the disk, the center hole and mounting screw do not impact the performance of the SWGT.

The sapphire disk was enclosed within a resonance cavity comprising of two pieces of gold-plated, oxygen-free, high-conductivity copper. These pieces were sealed

together with a silicone o-ring. Holes were drilled in the cavity for mounting the disk, admitting coaxial microwave cables, and a vacuum line. The microwave cables are mounted in the WGH direction (WG indicates a whispering gallery mode and H refers to the dominant component of the electromagnetic field perpendicular to the  $c$ -axis of the crystal). The original design did not allow for the cavity to be evacuated. However, problems arose during the first set of measurements that were attributed to moisture; therefore, a vacuum line was added to continuously pump the cavity during the subsequent measurements.

During the preliminary measurements (when the resonance cavity containing air was sealed), water seeped through the o-ring seal into the resonance cavity while the SWGT was immersed in an ice melting point (ice MP, 0°C) overnight. Some water condensed on or near the synthetic sapphire disk, causing a drift in the whispering gallery resonance frequencies by the equivalent of 300 mK and a reduction in the  $Q$ -factors. Upon drying the cavity, we found that the drifts in  $f_0$  and  $Q$  were reversible. As an additional precaution, the SWGT was placed in a metal foil bag to prevent water from contacting the cavity. The continuous evacuation of the SWGT contained in the metal foil bag gave an increase of 0.002% in resonance frequencies at 0°C, and an increase in the  $Q$ -factors of 1%. More importantly, the repeatability of  $f_0$  improved from 10 mK to less than 2 mK. Additionally, the thermal cycling instability of the SWGT at 0°C was reduced from 300 mK to 1 mK. All results in this article reflect the continuously-evacuated SWGT-T1 design.

In order to reduce the number of coupling connectors and the physical size of the SWGT, the coaxial microwave cables were soldered directly into the cavity. The lengths of the antennae were chosen to optimize the whispering gallery resonances and reduce the spurious cavity resonances. We started with antennae that were 4-mm-long pins. The pin length was reduced incrementally to 0 mm (flush with the cavity wall). Two results were observed. First, the  $Q$ -factors of the spurious cavity resonances were reduced to less than 10,000. Second, the whispering gallery resonance  $Q$ -factors were increased to as much as 90,000. Recessing the antenna into the cavity wall led to a reduction in the whispering gallery  $Q$ -factors. The current SWGT design uses the 0 mm antenna length.

Figure 3a shows an open SWGT-T1 resonance cavity with the mounted  $\alpha$ -Al<sub>2</sub>O<sub>3</sub> disk (8.8 mm diameter), microwave cables, and the 0 mm length antenna. Figure 3b shows the sealed SWGT-T1 with the added vacuum line.

#### 4 Experimental Measurements

The first goal of the measurements was to quantify the resolution, stability, and repeatability of the SWGT at 0°C. The second goal was to measure the temperature dependence of several whispering gallery resonance frequencies as a function of temperature. The experiments performed included resolution and repeatability determinations at 0°C, thermal cycling between 0°C and 50°C, and calibration from 0°C to 100°C. Only the largest SWGT (SWGT-T1) results are reported in this article. The SWGT-T1 was handled with the care normally associated with an industrial thermometer, and not with the specialized care that an SPRT receives.

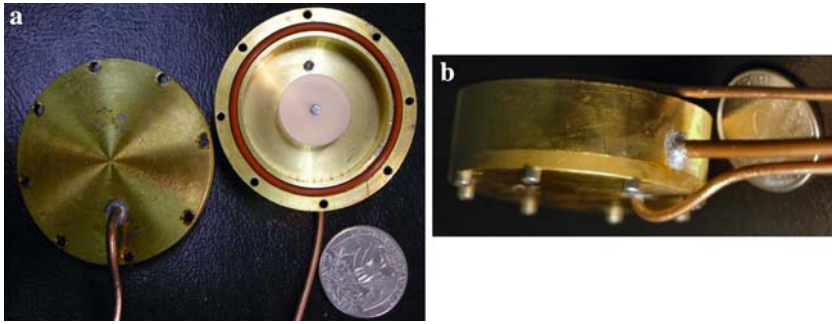


**Fig. 3** (a) Open SWGT-T1 resonance cavity with the mounted  $\alpha$ - $\text{Al}_2\text{O}_3$  disk (8.8 mm diameter), microwave cables, and the 0 mm length antenna, and (b) sealed SWGT-T1 with the added vacuum line

The SWGT measurement system consisted of an Agilent Model N5230A<sup>†</sup> network analyzer (10 MHz to 20 GHz) with a Stanford Research Systems Model FS725 of 10 MHz rubidium frequency standard. An NIST ITS-90 calibrated SPRT with an ASL F18 resistance-ratio bridge was used to determine the comparison bath temperatures. The water bath temperature determination uncertainties ( $k=1$ ) do not exceed 1 mK [15]. The 0 °C realization uncertainty ( $k=1$ ) is 1 mK [16].

Five whispering gallery modes with nominal resonant frequencies ranging from 14.4 GHz to 19.1 GHz and with  $Q$ -factors, respectively, ranging from 20,000 to 90,000 were measured. From the 0 °C measurements, it was determined that the frequency stability of any of the five resonance modes was equivalent to 0.2 mK. The resonant line shape function for the frequency distribution of energy in a microwave cavity is used to fit the SWGT resonance frequency curves to determine  $f_0$  (center frequency) and  $g$  (half-width) [14]. Figure 4 shows a residual plot from a fit to one of the SWGT-T1 resonance frequency curves. On the basis of average of a fit to the five  $f_0$  values, the uncertainty ( $k=1$ ) in determining  $f_0$  is less than 0.05 mK.

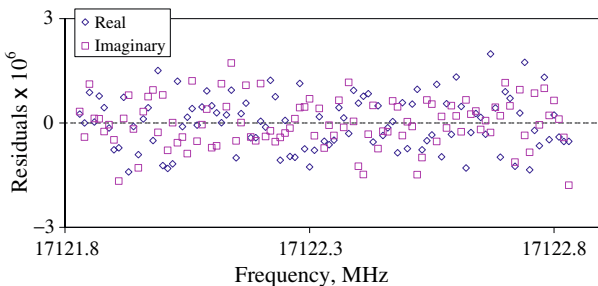


**Fig. 4** Plot of the fit residuals following a determination of  $f_0$  (center frequency) for one of the SWGT-T1 resonance frequency modes

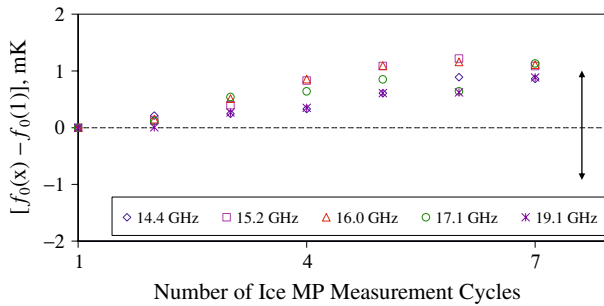


**Fig. 5** SWGT ice MP repeatability when thermally cycled between the ice melting point ( $0^{\circ}\text{C}$ ) and ambient. The legend gives the nominal  $f_0$  values obtained at  $0^{\circ}\text{C}$ . The arrows indicate the  $0^{\circ}\text{C}$  realization uncertainty ( $k=1$ ). In the y-axis label, the integer argument  $x$  indicates the cycle; thus,  $f_0(1)$  refers to the first  $0^{\circ}\text{C}$  measurement

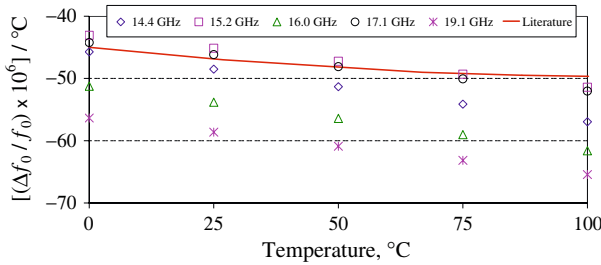
#### 4.1 Ice Melting Point ( $0^{\circ}\text{C}$ ) Repeatability

As seen in Fig. 5, the  $0^{\circ}\text{C}$  repeatability measurements were determined by thermally cycling SWGT-T1 between ambient and  $0^{\circ}\text{C}$  seven times. Prior to measurement, the SWGT-T1 thermometer was packed at a depth of 32 cm into the ice melting point for 30 min to achieve thermal equilibrium at  $0^{\circ}\text{C}$ . The legend gives the nominal  $f_0$  value obtained at  $0^{\circ}\text{C}$  for each measured whispering gallery mode. The SWGT-T1 shows an average drift rate of 0.18 mK per thermal cycle. After the fifth thermal cycle, the drift rate decreases to 0.08 mK per thermal cycle.

#### 4.2 SWGT-T1 Frequency Versus Temperature Model

To develop a calibration model for the SWGT, the resonance frequencies of the same five whispering gallery modes of SWGT-T1, as used in Sect. 4.1, were measured at 0, 25, 50, 75, and  $100^{\circ}\text{C}$ . From the results, we determined the fractional change in  $f_0$  as a function of temperature  $[(df_0/dT)/f_0]$  for each of the five modes (i.e., the sensitivity). Figure 6 shows the results for the five modes and the available literature values for the  $f_0$  versus  $t$  sensitivity. The literature curve is fit through the experimentally derived values from previously published values for a single mode [1–10]. The literature  $(df_0/dT)/f_0$  values quadratically change from  $-45 \times 10^6 \text{ }^{\circ}\text{C}^{-1}$  at  $0^{\circ}\text{C}$  to  $-50 \times 10^6 \text{ }^{\circ}\text{C}^{-1}$  at  $100^{\circ}\text{C}$ . For SWGT-T1, the  $(df_0/dT)/f_0$  values vary systematically as a function of measured whispering gallery mode. For example, the 14.4 GHz  $(df_0/dT)/f_0$  values range from  $-45 \times 10^6 \text{ }^{\circ}\text{C}^{-1}$  at  $0^{\circ}\text{C}$  to  $-54 \times 10^6 \text{ }^{\circ}\text{C}^{-1}$  at  $100^{\circ}\text{C}$ , and the 19.1 GHz  $(df_0/dT)/f_0$  values range from  $-57 \times 10^6 \text{ }^{\circ}\text{C}^{-1}$  at  $0^{\circ}\text{C}$  to  $-64 \times 10^6 \text{ }^{\circ}\text{C}^{-1}$  at  $100^{\circ}\text{C}$ .

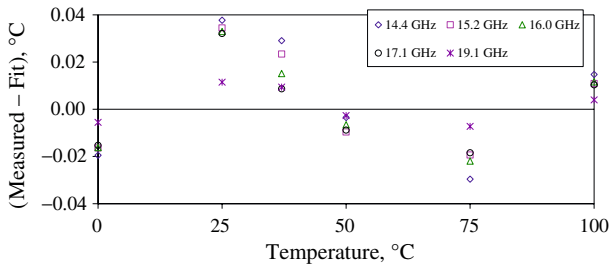
In an attempt to understand how the SWGT-T1  $f_0$  values for each of the five modes change as a function of temperature, a quadratic function and a cubic function were fit to the  $f_0$  values measured at 0, 25, 50, 75, and  $100^{\circ}\text{C}$ . An additional temperature ( $37^{\circ}\text{C}$ ) was measured to quantify the interpolation uncertainty of the fit.



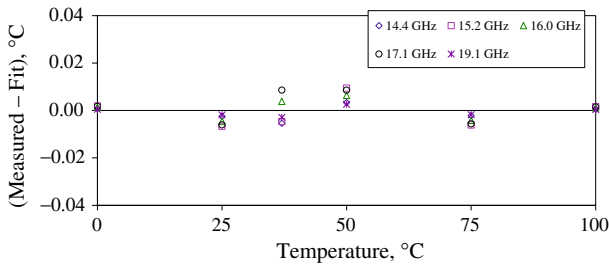
**Fig. 6** SWGT-T1  $f_0$  versus  $t$  sensitivity for five measured whispering gallery modes and previously published values (single mode) in Refs. [1–10]

Figure 7 shows the residuals of the quadratic fit at six temperatures for each of the five modes. Figure 8 shows the residuals of the cubic fits for the same data sets as shown in Fig. 7.

For the quadratic fit, the standard deviation of the residuals decreased from 27 mK to 8 mK as a function of increasing mode (e.g., 14.4–19.1 GHz). The range in the 37 °C  $f_0$  results is 21 mK with a decrease in the difference from the fit, as a function of increasing mode. The 19.1 GHz mode, where the  $Q$  factor is the highest, shows the best fit with an interpolation error of 8 mK at 37 °C. The quadratic residuals in Fig. 7 show a structure that suggests the use of a cubic function (see Fig. 8).



**Fig. 7** SWGT-T1 quadratic fit residuals for each whispering gallery mode. The 37 °C  $f_0$  is a redundant measurement point to quantify the uncertainty of the fit



**Fig. 8** SWGT-T1 cubic fit residuals for each whispering gallery mode. The 37 °C  $f_0$  is a redundant measurement point to quantify the uncertainty of the fit



The Fig. 8 cubic fit residuals show an expected improvement over that of the quadratic fit residuals. The standard deviations of the residuals range from 2 mK to 6 mK and are not correlated as a function of increasing mode (e.g., 14.4–19.1 GHz). The 37 °C  $f_0$  interpolation error for all five measured modes gave a range of 14 mK with no correlation in the results as a function of increasing mode number.

Several models [e.g.,  $f_0(1+1/(2Q))$ ,  $f_0(1+1/Q^2)$ ] were tried in an unsuccessful attempt to normalize the results (a model using frequency and  $Q$  should be independent of mode number), and develop a single reference function for all five modes. Further measurements with different SWGTs and antenna configurations are necessary to understand how to normalize the results with respect to the  $f_0$  and  $Q$ -factor values.

## 5 Conclusions

The current version of the NIST SWGT is a promising thermometer that achieved a measurement uncertainty ( $k=1$ ) of 10 mK from 0 °C to 100 °C for any of the five measured whispering gallery resonance modes. This performance approaches the capabilities of most industrial resistance thermometers. The calibration results and associated uncertainty components are particular to the prototype SWGT-T1; they do not imply intrinsic interchangeability of SWGT devices.

We plan to determine the capabilities of an SWGT as a function of design, size, and temperature range. The next steps include fabricating a hermetically-sealed SWGT (e.g., no vacuum system), and determining the smallest practical size, the useable temperature range with associated measurement uncertainties, and a possible reference function that is mode independent. Following the optimization of the SWGT, we will study the long-term drift of an SWGT in regular use.

If the SWGT can be reduced in size to a diameter of less than 3 cm, and maintain a temperature reproducibility <10 mK over a temperature range from –196 °C to 500 °C, then the thermometer will be competitive with an SPRT. The cost of a network analyzer is comparable to that of a resistance ratio bridge for an SPRT. However, knowing the nominal whispering gallery mode  $f_0$  values, it is possible to build an SWGT measurement system at a fraction of the cost of a network analyzer. If the SWGT proves to be a robust alternative to the fragile SPRT, then the impact on the type of thermometer used in industry will be significant in terms of calibration costs. Additionally, areas (e.g., chemical processes, plastic fabrication, aerospace, remote weather stations) that need better temperature measurement uncertainty (<10 mK) and are limited by current SPRT technology can potentially be addressed by a SWGT.

**Acknowledgment** The author gratefully acknowledges the technical input from Dean Ripple and Mike Moldover and fabrication assistance from Wyatt Miller. This project was funded by the NIST CSTL Exploratory Research program.

## References

1. E.N. Ivanov, D.G. Blair, V.I. Kalinichev, IEEE T. Microw. Theory **41**, 632 (1993)
2. M.E. Tobar, J. Krupka, E.N. Ivanov, R.A. Woode, J. Phys. D: Appl. Phys. **30**, 2770 (1997)

3. V. Giordano, Y. Kersalé, O. di Monaco, M. Chaubet, *Eur. Phys.-J. Appl. Phys.* **8**, 269 (1999)
4. V. Giordano, R. Barhaila, D. Cros, G. Duchiron, *Proceedings of the EFTF-IEEE IFCS Joint Meet.*, (Micropolis, Besançon, France 1999), pp. 593–596
5. I. Lajoie, R. Barhaila, Y. Kersalé, D. Cros, D. Duchiron, V. Giordano, *Electron. Lett.* **36**, 150 (2000)
6. M.E. Tobar, E.N. Ivanov, P. Blondy, D. Cros, P. Guillon, *IEEE T. Ultrason. Ferr.* **47**, 421 (2000)
7. M.E. Tobar, A.G. Mann, *IEEE T. Ultrason. Ferr.* **39**, 2 (1991)
8. E.N. Ivanov, D.G. Blair, V.I. Kalinichev, *IEEE T. Microw. Theory* **41**, 632 (1993)
9. G.J. Dick, J. Saunders, *IEEE T. Ultrason. Ferr.* **37**, 339 (1990)
10. C. McNeilage, J.H. Searls, E.N. Ivanov, P.R. Stockwell, D.M. Green, M. Mossammaparast, *IEEE UFFC Soc. Newsletter* (2005) and references therein
11. D.B. Minor, G.F. Strouse, *NCSLI Conference Proceedings*, Washington, DC (2005), [http://store.ncsli.org/Stabilization\\_of\\_SPRTs\\_for ITS\\_P741C42.cfm](http://store.ncsli.org/Stabilization_of_SPRTs_for ITS_P741C42.cfm)
12. R.J. Berry, *Metrologia* **15**, 117 (1980)
13. L.M. Belyaev (ed.), *Ruby and Sapphire* (Amerind Pub., New Delhi, 1980)
14. J.D. Jackson, *Classical Electrodynamics* (John Wiley & Sons, New York, 1975)
15. G.F. Strouse, B.W. Mangum, C.D. Vaughn, E.Y. Xu, A New NIST Automated Calibration System for Industrial Platinum Resistance Thermometers, *NISTIR 6225* (1998)
16. B.W. Mangum, Reproducibility of the Temperature of the Ice Point in Routine Measurements, *NIST Tech. Note 1411* (1995)